STERILIZATION OF MEDICAL PRODUCTS

Volume VI

Editor:

Robert F. Morrissey, Ph.D.
Johnson & Johnson
Sterilization Sciences Group
U.S.A.

Proceedings of the International Kilmer Memorial Conference on the Sterilization of Medical Products

Brussels, Belgium
June 13-15, 1993

ISBN 0-9221317-46-8

Polyscience Publications Inc.
Morin Heights, Canada

Printed in Canada

ESR-Based Analysis in Radiation Processing

William L. McLaughlin*, Marc F. Desrosiers*, and Michael C. Saylor**

*National Institute of Standards and Technology, U.S.A.
**Dunn-Loring, Virginia, U.S.A.

Introduction

Electron spin resonance (ESR)[1] analysis of irradiated materials, especially polyolefins, polystyrene, and specialty resins, is a well-established technology (10,11,12). Most studies of irradiated polymers by ESR spectrometry have been directed to the understanding of radiation damage effects (28,51) and to ways of limiting the damage by the addition of certain organic lubricants and antioxidants (5,72). Work by Morita et al (44) has demonstrated that it is possible to explain by ESR analysis the reaction kinetics caused by radiolytic peroxy, methoxy, and alkyl radicals in polymers, as well as the protective role played by light stabilizers (e.g., hindered-amine polycyclic compounds) in polymers. ESR can also be used to register images of absorbed dose distributions in key polymers such as polypropylene (44). The most significant radiation effect in plastics, and in both organic and inorganic solid-state substances, is damage caused largely by radiation-induced free-radicals that can have a long latency period. These effects often result in the eventual coloration, embrittlement, and other losses of mechanical strength and durability of these materials.

The use of ESR for analysis of stable free radicals as a means of radiation dosimetry also has a long history (6,7,9,56,60). In spite of its birth more than 30 years ago, however, ESR dosimetry still has to prove itself as an established, commercially-viable method of measurement for industrial processing by ionizing radiation and for other dosimetry purposes. As witnessed by three recent sequential international symposia on ESR dosimetry (with a fourth scheduled for Munich in 1995) (20,32,58), the subject has proven to be broad and comprehensive. It covers not only high-dose dosimetry and standard measurement services for industrial processing applications (radiation sterilization of medical devices and pharmaceuticals and food irradiations), but also dosimetry review for radiation emergencies (e.g., Chernobyl), clinical dosimetry (e.g., teletherapy treatment planning), bone dosimetry in nuclear medicine, dating in archeology, geology, and paleontology, and radiation effects and imaging in a variety of materials (42). Figure 1 gives a chart of applications and systems now under investigation at the U.S. National Institute of Standards and Technology.

---

[1] In many texts referred to as electron paramagnetic resonance (EPR).

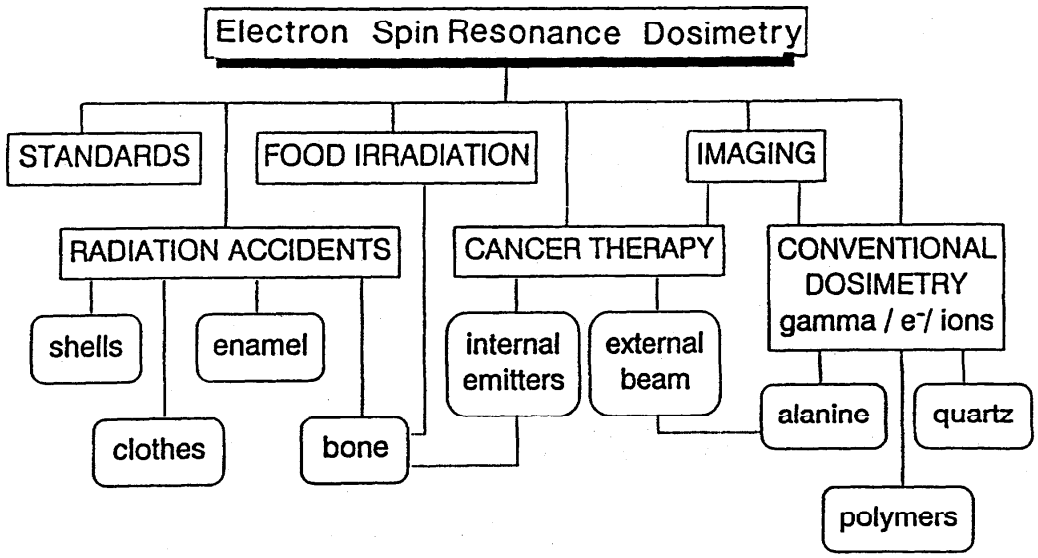

Figure 1. Applications and Examples of Systems for ESR Dosimetry Carried Out at the U.S. National Institute of Standards and Technology

One important reason for the burgeoning interest in this many-faceted approach to practical dosimetry is the very broad dynamic range that is achievable by ESR spectrometry, generally stated to be 10^{-1} to 10^{8} Gy (41).[2] Alanine/ESR dosimetry is one of the most important methods, having an operable dose range of 10^{0}-10^{5} Gy (56,57,59,71).

Successes have been demonstrated with alanine/ESR in several quarters: 1) the International Atomic Energy Agency's International Dose Assurance Service (IAEA's IDAS), first instituted jointly by the IAEA and the German Gesellschaft für Strahlen-und Umweltforschung (GSF) in 1985 (48,49,57); 2) the ESR alanine dosimeter reference service begun in 1991 at the U.K. National Physical Laboratory (NPL) in Teddington (61); and (3) similar measurement services administered by the Italian Istituto Superiore di Sanità (ISS) in Rome (59), by the French Laboratorie Primaire des Rayonnesment Ionisants/Bureau National de Metrologie (LPRI/BNM) in Gif-sur-Yvette (62), and the Japan Atomic Energy Research Institute (JAERI) in Takesaki (36).

There are, however, four distinct limitations that have restricted its universal use by industry. These limitations have been: 1) the capital expense of the ESR spectrometer, which, until recently had a cost that was more than an order-of-magnitude greater than that of a conventional double-beam UV-visible spectrophotometer; 2) the lack of an easy-to-use ESR spectrometer that is dedicated to dosimetry; 3) the relatively high cost of individual dosimeter units; and 4) the absence of a supplier of mass-produced, widely-available, lower-cost, reproducible

[2] The unit of quantity *absorbed dose* is the named unit, *gray* (Gy), defined as 1 Gy ≡ 1 Jkg^{-1}. This unit is related to the older unit, rad, as 1 Gy = 1 rad, or 1 kGy = 100 krad = 0.1 Mrad.

batches of dosimeters. It is encouraging that these four limitations are now being rectified, and the overall costs are approaching those of conventional systems (see Table I and Figure 2) (3,37,40). In fact, the wide acceptance and potentially greater market for alanine/ESR in a number of dosimetry applications is driving the cost of the dosimetry-dedicated ESR spectrometer down to the same level as that of the top-of-the-line UV-*vis* spectrophotometer (see Table I).

Table I. Estimated Dosimetry Costs (U.S. Dollars)

Type	Cost per Dosimetry (in bulk)	Cost per Reader
Fricke	2	10-30 k
Ceric Cerious ("Compu-Dose")	2	0.5-3 k
PMMA (Harwell)	0.7	10-30 k
RCD films (FWT)	0.13	2-30 k
RCD films (GAF)	0.05	2-30 k
Alanine	1 to 10	30-220 k

The details of the traditional ESR spectrometer are thoroughly described in the literature (2,40). It possesses an electromagnet equipped with a cavity that is usually operated in the microwave X-band with an external static magnetic field that is modulated at radio frequencies. The electron spin resonance absorption is measured by sweeping the external magnetic field strength over prescribed limits, depending on the paramagnetic properties of the test sample. Standardizing the ESR absorption intensities can be accomplished by measurement of a standard sample having a stable and relatively simple ESR signal (e.g., O_2-depleted charcoal). The ESR analysis is generally carried out with the small dosimeter sample fitting into a quartz capillary tube (typical inner diameter ~0.5 cm), which is inserted at a fixed, repetitive position in the magnetic field (see Figure 3). Following the magnetic field sweep, the computerized console then stores and displays the relevant data, including the ESR absorption spectrum, usually as its first derivative (see Figure 4).

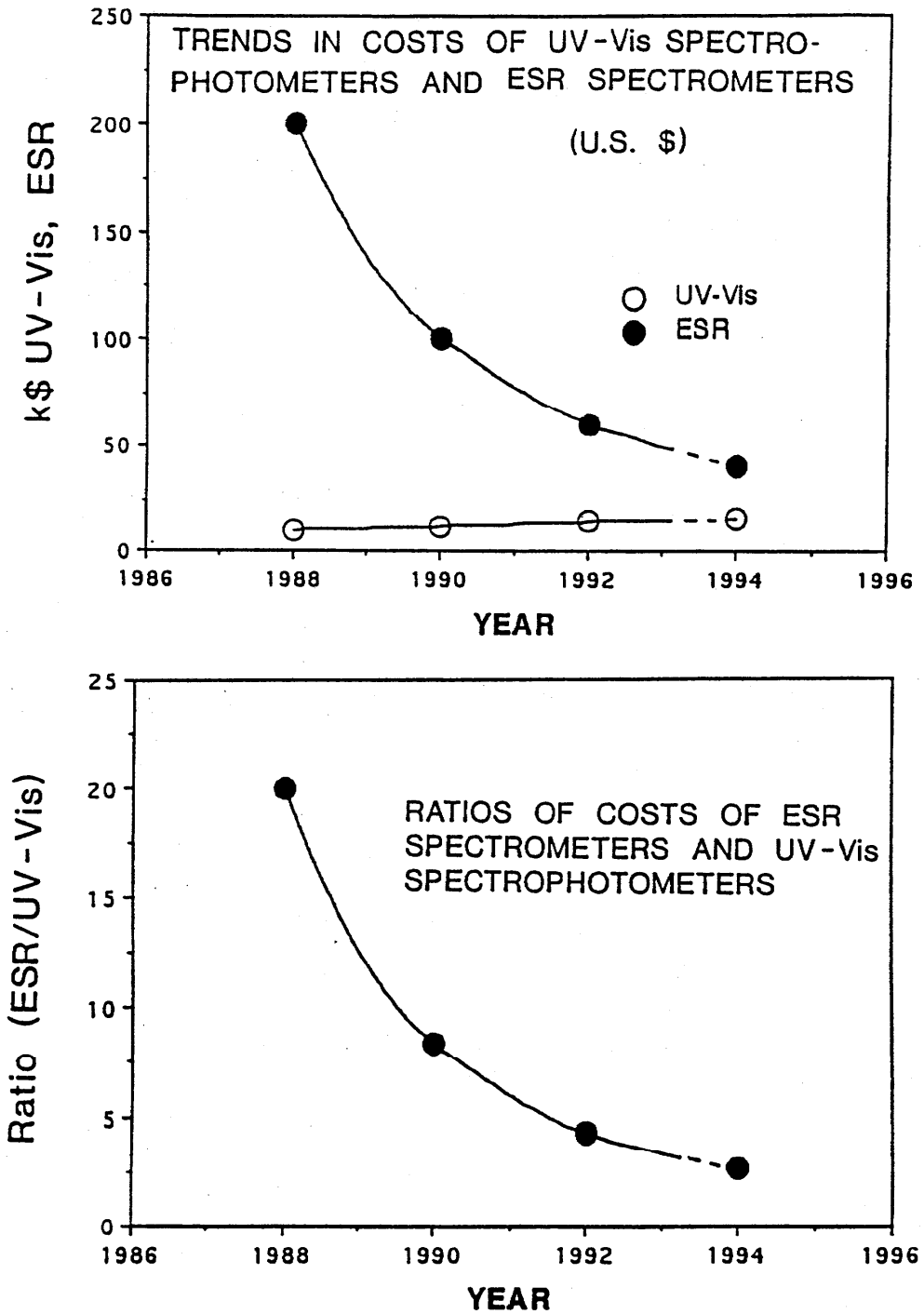

Figure 2. Cost Trends (top) Since 1988 for ESR Spectrometers and UV-Visible Spectrophotometers and Their Ratios (bottom)

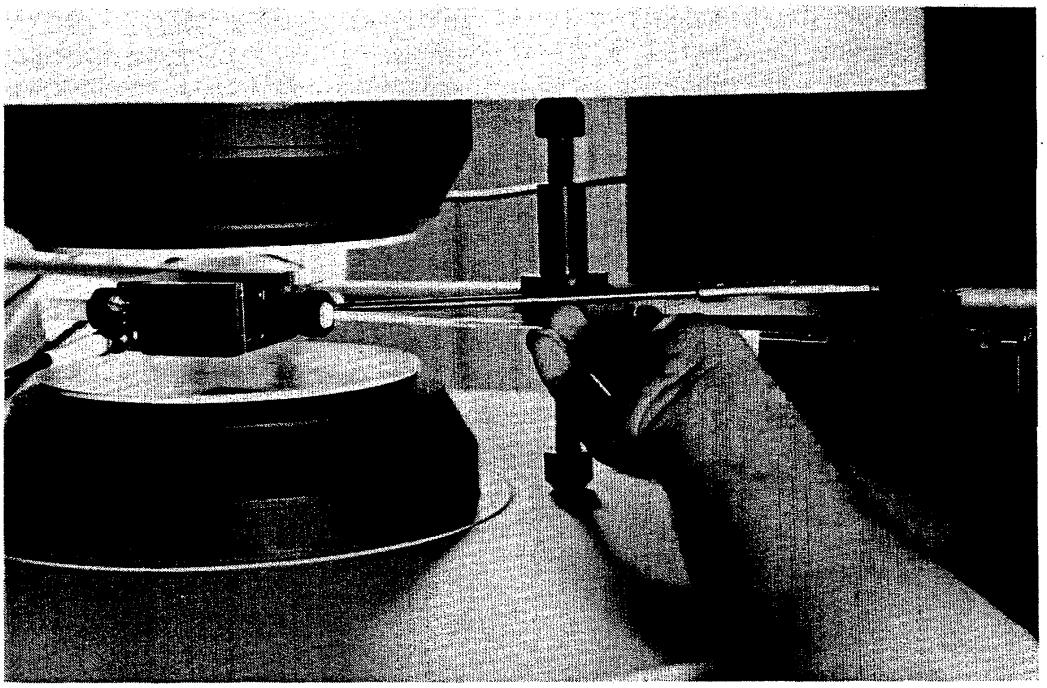

Figure 3. The Placement of a Quartz Sample Tube in the Microwave Cavity Between the Electromagnet Dipoles of the ESR Spectrometer

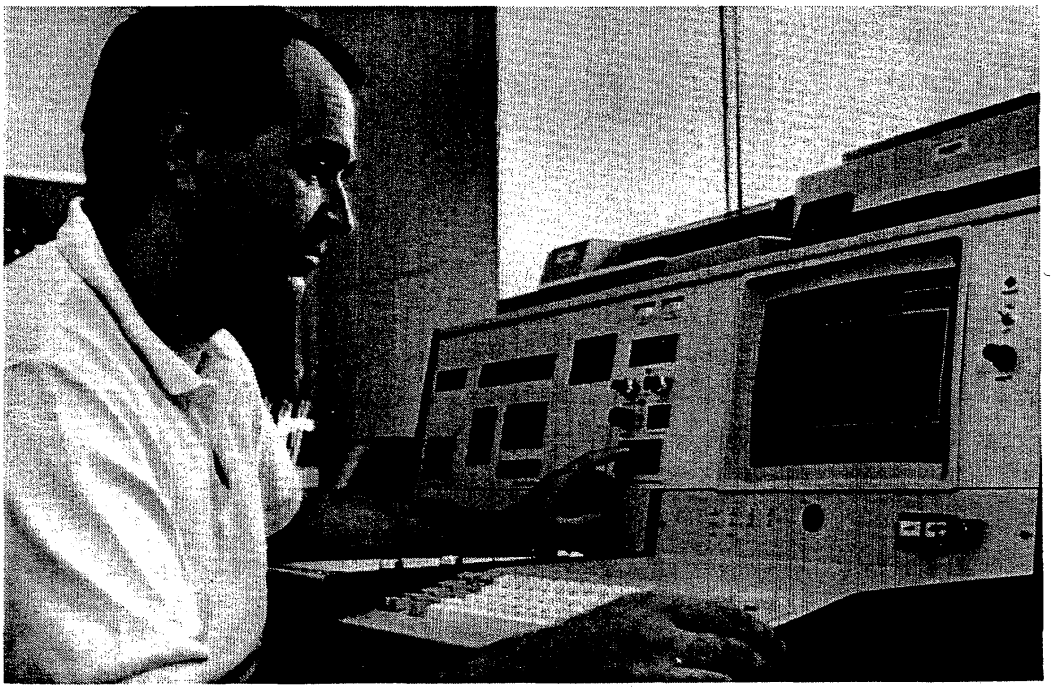

Figure 4. The Reading of an ESR Spectrum of an Alanine Sample at the Console of the Spectrometer

At present, the most commonly used ESR dosimeter is based on microcrystalline L-α-alanine, $CH_3CH(NH_3^+)CO_2^-$, which is usually held in a polymeric binder such as low molecular weight polyethylene or paraffin, polystyrene, or ethylene-propylene rubber. The mixture is made into a rod, pellet, or, for some applications, a film (34,36) or cable (15), that can be cut into convenient sizes (see Figure 5). The chemical reaction involves the radiation-induced deamination of the zwitterions into the radical anions (39):

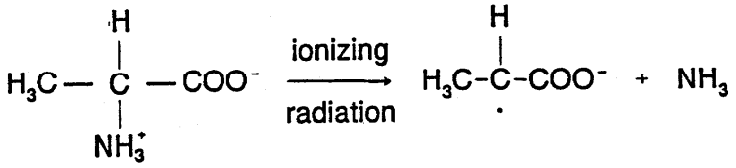

which act as stable paramagnetic centers in the solid state.

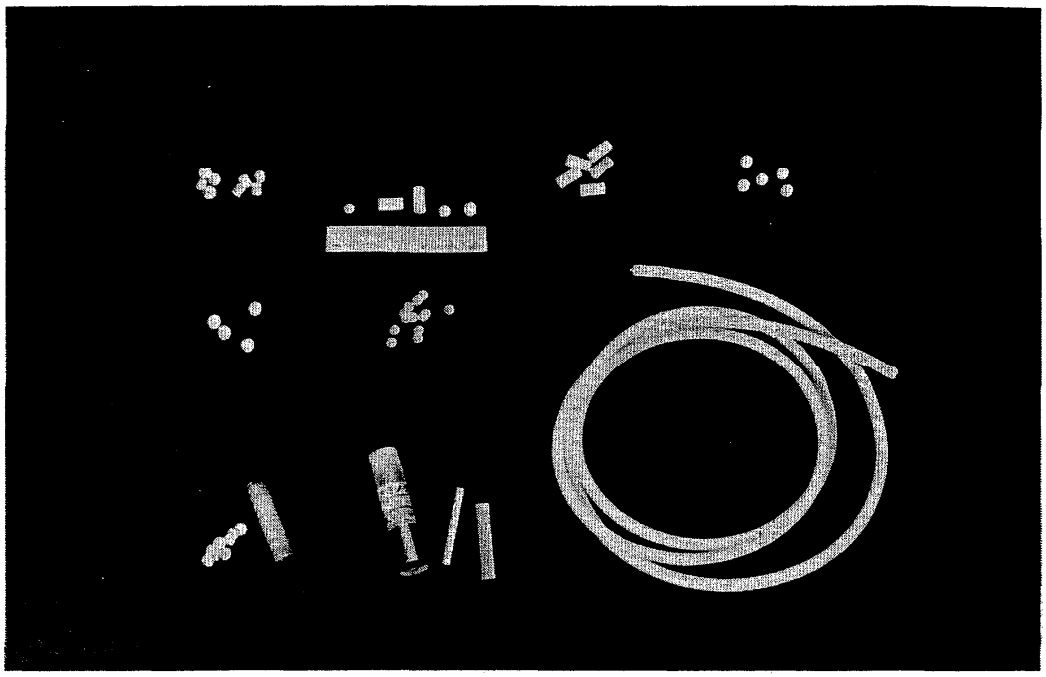

Figure 5. Examples of Different Kinds of Alanine/Polymer Dosimeters, Including Pellets, Rods, Film Pieces, and Cable

The primary aim of this paper is to review the status of alanine dosimetry, as well as the use of other suitable materials compatible with ESR analysis, for applications (especially those of radiation processing) over a broad range of absorbed doses. We shall also present a perspective for the future of this dosimetry method and its relevance for a variety of radiation processing applications. Paramount to our expectations are diminished costs, improved accuracy and precision, and the introduction of better, more widely available dosimeters and readout techniques (e.g., imaging of two- or three-dimensional dose distributions).

Basis of ESR for Dosimetry

Upon irradiation of the amino acid, L-α-alanine, or other materials (e.g., sugars, silica, certain polymers), stable free radicals may be created. These radicals are in the form of paramagnetic centers[3] consisting in this case of unpaired electrons that are trapped, for example, by impurities or crystalline matrices. This population of stable centers is usually proportional to the absorbed dose. The medium is then placed in the ESR spectrometer cavity and subjected to the strong, swept magnetic field. The sample cavity is operated at microwave frequencies (using the X-band at a fixed frequency within the range 9 to 10 GHz) with a perpendicular external static field modulated at a certain radiofrequency (RF) usually between 50 to 100 kHz. In this crossed magnetic field, the medium undergoes microwave absorption that is characteristic of the particular gyromagnetic properties of interactions between the precessing magnetic movement of the electron spin and the surrounding molecular system. This absorption is measured usually by a silicon-based Schottky diode detector acting as a microwave rectifier, and, for most dosimetry applications, is registered as its first derivative (see Figure 6).

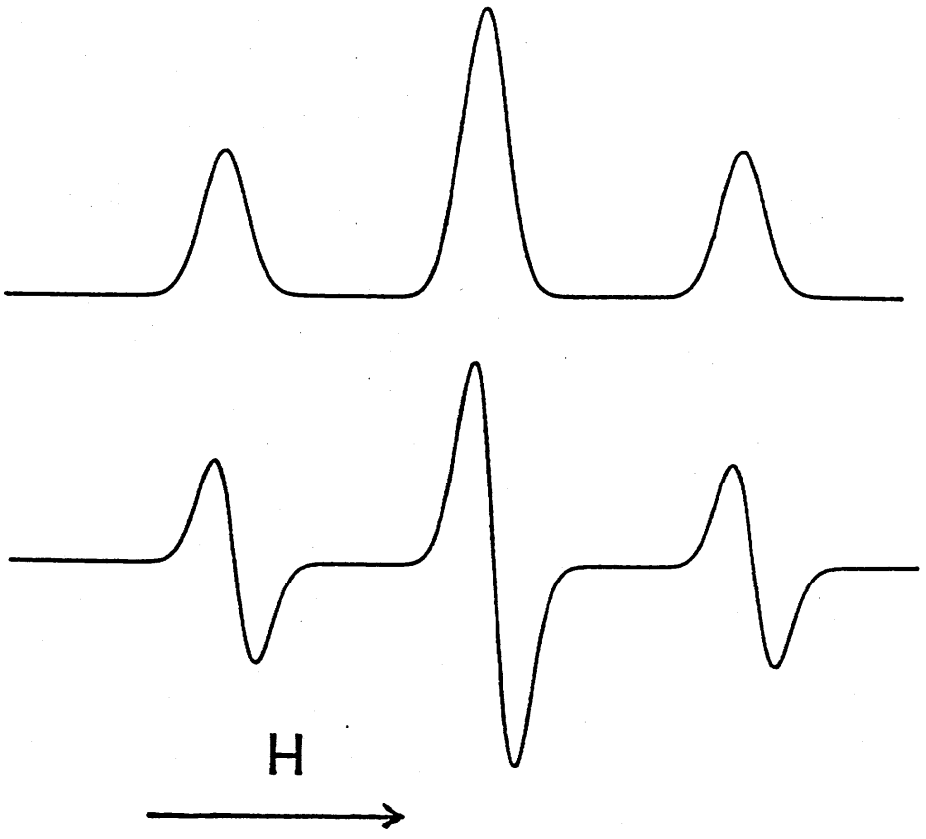

Figure 6. Examples of a Simple ESR Absorption Spectrum (top) and Its First Derivative (bottom)

[3] Paramagnetic centers may also exist as free radicals trapped by transition metals, rare earth ions, or organic chelates or clathrates.

As illustrated in Figure 7, the splitting of the electron spin states allows permitted magnetic dipole transitions (2), which the unpaired electron spin system experiences in the crossed steady (H) and RF (H_1) magnetic fields as a splitting of Zeeman energy states ($M_s = +½$ and $-½$). The line energy absorption is such that the following resonance condition is satisfied for the energy-level separation, ΔE:

$$\Delta E = h\nu = g\mu_\beta H$$

where h is Planck's constant, ν is a selected frequency giving a certain paramagnetic absorption, g is the dimensionless Landé spectroscopic splitting factor, μ_β is the constant Bohr magneton ($\mu_\beta = 9.2741 \times 10^{-22}$ J T^{-1}), and H is the swept magnetic field strength in tesla (T).[4] The value of g is typically about 2, and for the free electron $g_e = 2.00232$. The first-derivative spectral amplitude of the main peak-to-peak spread is proportional to the concentration of paramagnetic species, and the absorption spectral shape and the resonant region in the swept field depend on the hyperfine coupling between the unpaired electron and the magnetic moment of the surrounding nuclei. For ESR dosimetry readings, the choice of the magnetic sweep depends on the kind of paramagnetic center being observed and on its molecular environment; for example, the amino acid, alanine, at room temperature, may require a 20-mT full sweep, while the radiation-induced E′ center in quartz (SiO_2) is encompassed by a 0.2-mT sweep.

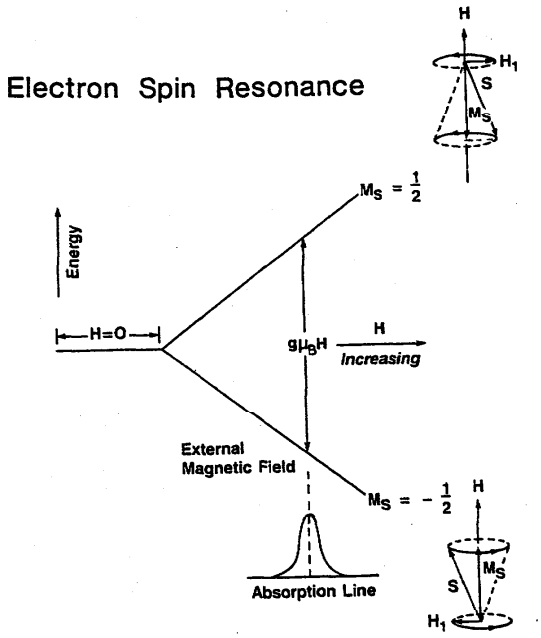

Figure 7. Energy Level Diagram Showing Zeeman Splitting for a Simple Free Electron Spin System in Crossed Steady (H) and Radiofrequency (H_1) Magnetic Fields (2)

[4] The unit of the quantity, *magnetic field strength*, is the named unit, tesla (T), where tesla is related to the order unit, gauss (G), as $1\ T = 10^4\ G$.

Table II. ESR Dosimetry Systems (Organic)

Dosimetry Material	Binder Material	Form	Dose Range p (Gy)	Sample Reference
L-α-alanine ($C_3H_7NO_2$)	polymer (e.g., paraffin)	rods, pellets, films	10^0–10^5	56
D-α-sucrose ($C_{12}H_{22}O_{11}$)	polymer (e.g., paraffin)	rods, pellets, powder	10^{-1}–10^4	4
D-α-lactose ($C_{12}H_{22}O_{11}\cdot H_2O$)	polymer (e.g., paraffin)	rods, pellets, powder	10^2–10^5	53
methyl viologen ($C_{12}H_{14}N_2$)	polymer (e.g., polyvinyl alcohol)	films	10^2–3×10^5	50
tris(hydroxymethyl aminomethane ($C_4H_{11}NO_3$)	—	pellets, powder	5–10^4	53
cellulose $(C_{12}H_{20}O_{10})_n$	—	wafers, films	10^3–5×10^5	70
triphenylmethane dyes $(C_{20}H_{18}N_4)_n$	polymer (e.g., polyvinyl butyral)	films	10^3–10^5	68
polyvinyl alcohol $(C_2H_4O)_n$	—	films, powder	10–10^5	21
polytetrafluoroethylene $(C_2F_4)_n$	—	rods, films, powder	10^2–10^6	35

Dosimetry Systems

Many solid materials show relatively stable paramagnetic properties when subjected to ionizing radiation. Tables II and III list, respectively, organic and inorganic materials, their usual form for dosimetry, typical dose ranges, and a sample reference for each. It can be seen from these listings that a very wide absorbed dose range can indeed be measured (10^{-1}-10^{8} Gy) by ESR analysis.

Table III. ESR Dosimetry Systems (Inorganic)

Dosimeter Material	Form	Dose Range (Gy)	Sample Reference
quartz (SiO_2)	glass, powder	10^4–10^8	69
magnesium orthosilicate (Mg_2SiO_4:Tb)	powder	5–3×10^3	8
magnesium sulfate ($Mg\ SO_4$)	powder	10^0–10^5	45
lithium fluoride (LiF:Mg,Ti)	powder	10^0–10^5	23
bone, hydroxyapatite ($Ca_{10}(OH)_2(PO_4)_6$)	powder, solid pieces	10^0–10^4	63
dental enamel, hydroxyapatite ($Ca_{10}(OH)_2(PO_4)_6$)	powder, solid pieces	10^{-1}–10^4	1,54

The radiation-induced first-derivative ESR spectra, with values of the g-factor centered at absorption bands where the ESR peak-to-peak signal can be measured for dosimetry is shown for the amino acid, L-α-alanine and the sugar, D-lactose, in Figure 8 and for the polymer, cellulose, and crystalline quartz (SiO_2), in Figure 9. On the right side of Figures 8 and 9 are the dosimetry response curves in terms of the ESR signal amplitude as a function of dose. These response functions illustrate the broad dose range of ESR analysis for passive dosimetry. The relatively broad response for the alanine/ESR system is illustrated in Figure 10, where typical dose ranges for several high-dose dosimeters are charted. It should be pointed out that the alanine/ESR system can provide measurements of doses covering not only those in the sterilization range (10^4–5×10^4 Gy), but also a dose region where precise and accurate dosimetry is especially needed, namely where both food irradiation and validation and dose-setting studies are made ($5 \times 10^2 - 10^4$ Gy). The reproducibility of alanine dosimetry has been reported by the NPL "Alanine Dosimeter Reference Service" in terms of a random uncertainty of $< \pm$ 1.2% (at 95% confidence level), with an overall uncertainty of $< \pm$ 3.0% (at 95% confidence level), for doses in the range $10^2 - 4 \times 10^4$ Gy (61). It has also been shown by Janovsk (34) that alanine film using polyethylene (vinyl acetate) as a binder covers the dose range up to 10^5 Gy (see Figure 11), with no variation between the response to gamma rays and electrons.

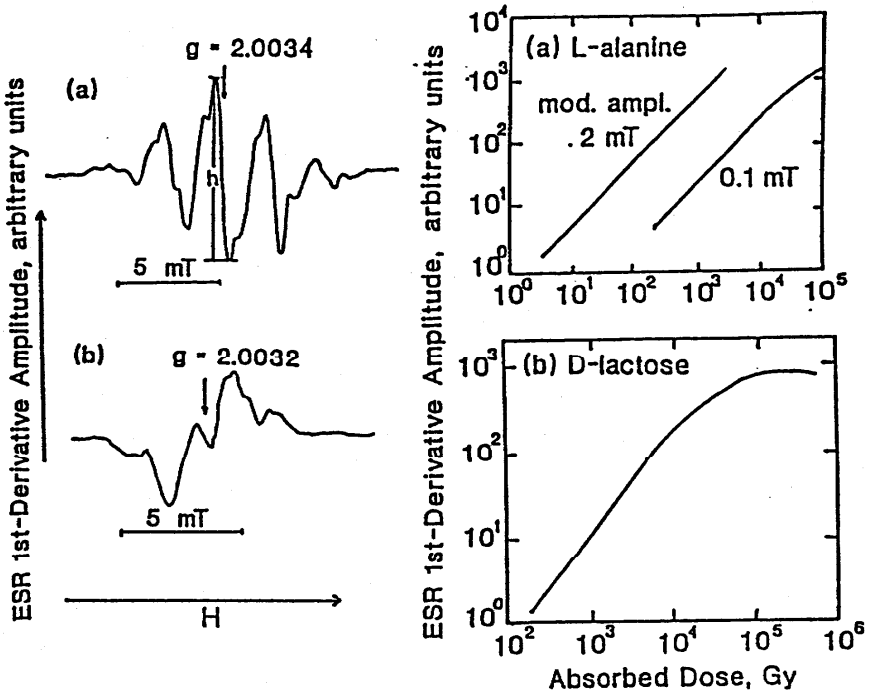

Figure 8. (Left) ESR First-Derivative Spectrum of Irradiated L-alanine (top) (The amplitude h is the usual measurement for dosimetry, which is a function of the absorbed dose) and D-lactose (bottom); (Right) Log-Log Plots of the Relative ESR Signal (h) Versus the Absorbed Dose (41)

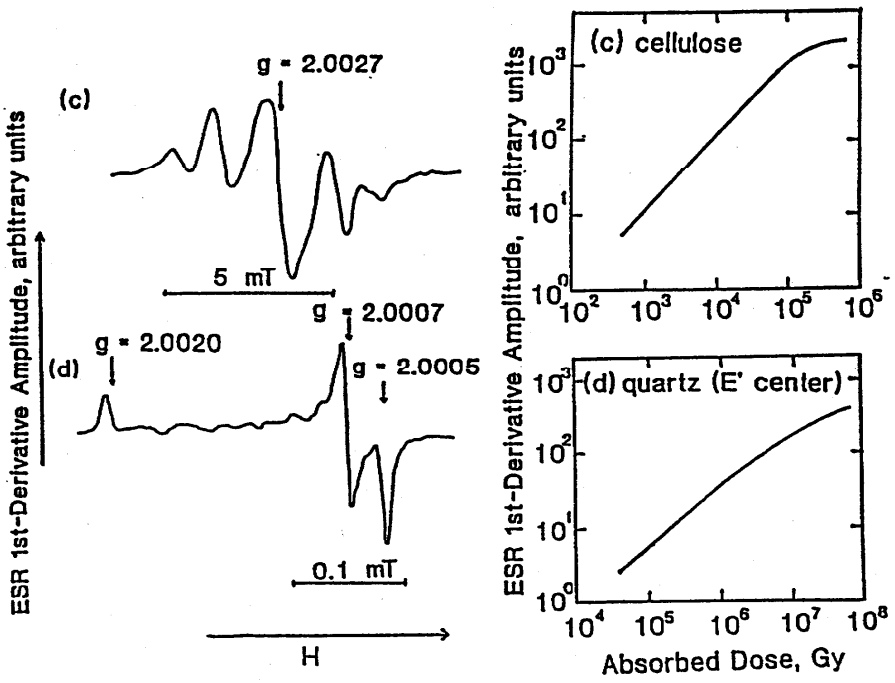

Figure 9. (Left) ESR First-Derivative Spectrum of Cellulose (top) and Quartz (bottom); (Right) Log-Log Plots of the Relative ESR Signal (h) Versus the Absorbed Dose (41)

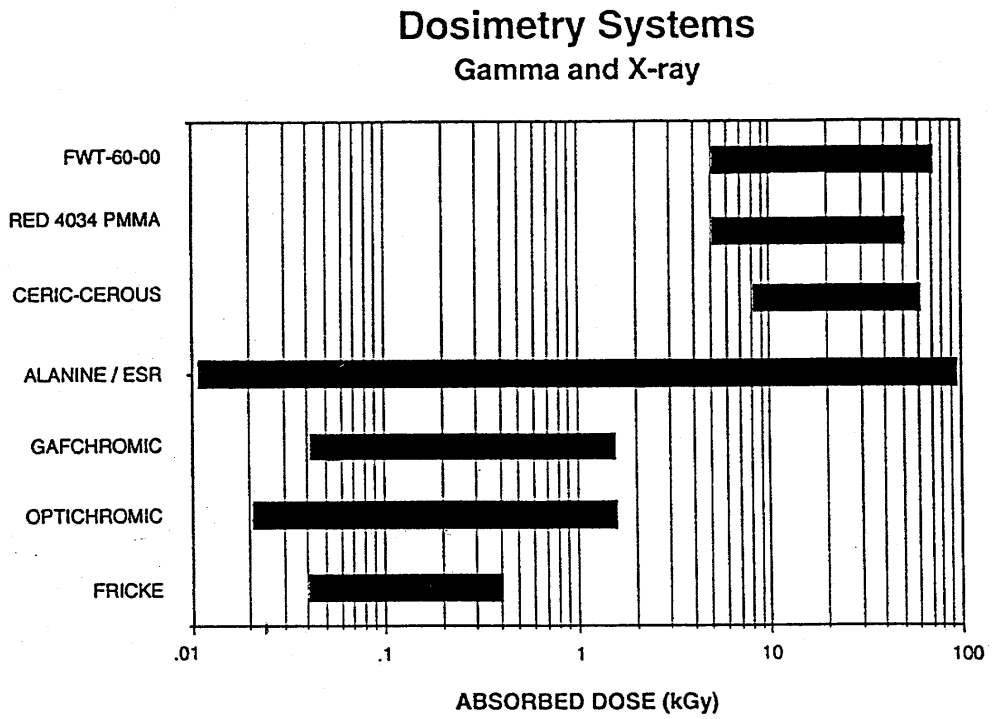

Figure 10. The broad dynamic absorbed dose range for alanine/ESR as compared with ranges for some other routine and transfer standard dosimetry systems commonly applied to medical device and food irradiation.

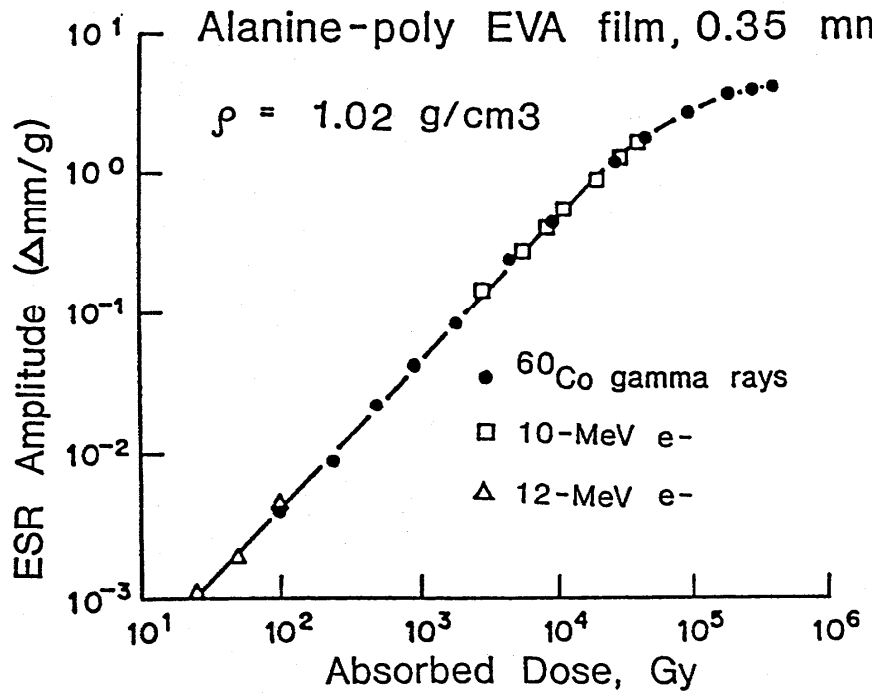

Figure 11. Response curve for a 0.35-mm thick alanine dosimeter using polyethylene-vinyl acetate as a binder (34). The film was irradiated over the dose range 2×10^1 – 5×10^5 Gy using gamma rays and electrons as indicated.

As will be discussed later, bone, tooth enamel, and skeletal tissue may also be used for dosimetry in several applications, including the detection of certain irradiated foods, nuclear medicine studies, and the dating of paleontological organic samples (20,32,58). The broad range covered by ESR analysis of the hydroxyapatite component of such tissues, compared with that for alanine, is illustrated in Figure 12, for several important applications.

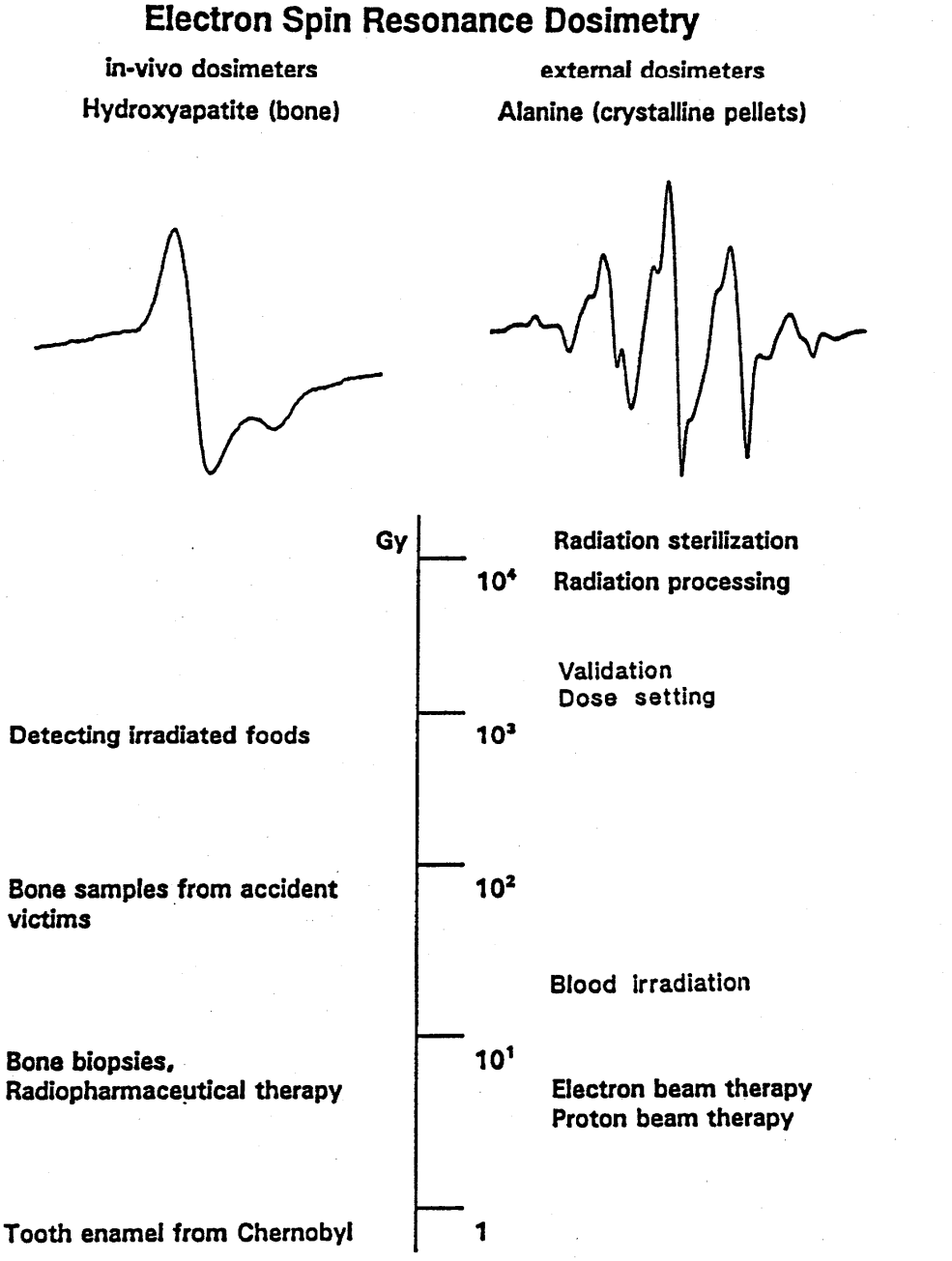

Figure 12. Examples of ESR Spectra for Bone and Alanine Dosimeters and Examples of Applications Over an Absorbed Dose Range 1 to > 10^4 Gy.

Alanine/ESR in Reference and Transfer Dosimetry

The main characteristics of alanine dosimetry systems are summarized in Table IV. For purposes of radiation processing dosimetry, some relevant properties that make alanine/ESR systems suitable for reference dosimetry and for interlaboratory transfer radiation measurements, considering the long delay times and different environmental conditions, are outlined in Table V.

Table IV. Alanine/ESR

- Dose range 10^0–10^5 Gy
- Long-term stability (years)
- Non-destructive analysis
- No read-out treatment
- High accuracy and precision
- Different geometries with a binder (pellets, rods, films, cables)
- Inexpensive materials
- Near-tissue-equivalence
- Relatively insensitive to ambient parameters (optimum conditions of storage: 50% ± 10% r.h.)

Table V. Alanine/ESR — Key Properties for Long-Term Dosimetry (At High Doses)

- Pre- and post-irradiation stability (permanent radiation effect, no rate dependence)
- Slight temperature dependence
- Slight photosensitivity
- Slight atmospheric effects (moisture, reactive gases, e.g., O_2, ozone)
- Inexpensive in large quantities, rugged, reproducible
- Large dynamic range (dose, dose rate)
- Easily calibrated

It was on the basis of these advantages that alanine/ESR dosimetry, as performed at GSF/Munich, was first selected as the IAEA International Dose Assurance Service system (48,49,57,59). This service by the IAEA is now operated as a mailed dosimetry evaluation procedure by the IAEA Seibersdorf Dosimetry Laboratory, and is presently extended to 31 institutes from 22 Member States. Calibrated alanine dosimeters are mailed, at Member State request, primarily to industrial and pilot-scale facilities, where they are irradiated along with reference or routine in-house dosimeters to doses in the range of 10^1–10^5 Gy. They are then returned to Seibersdorf and are evaluated, so that the measured dose can be compared to the nominal dose administered at the radiation facility. Since 1985 results have shown improved precision and accuracy of the evaluation of industrial radiation processing doses, as long as suitable care is given to controlling the geometry of dose delivery and monitoring of the temperature during irradiation is reported back to the dosimeter-issuing laboratory (42,48).

There are now attempts being made to develop alanine/ESR dosimetry for therapy level doses (10^1–10^2 Gy) (25,71). The question has even been asked as to whether this system, because of its key properties (see Table V), might replace the venerable Fricke dosimeter for clinical applications (25).

For such use at doses < 10 Gy, the main limitation for accurate dose assessment is the influence of the background signal in the region of the magnetic field where ESR absorption measurement is made. Figure 13 shows typical ESR spectra of unirradiated alanine/paraffin samples from five different batches, showing on the right the differences in apparent dose reading due to background signals (71). Because of this effect at low doses, it is necessary to use an empirical method of subtraction of this apparent dose (see Figure 14), which represents a significant effect at the therapy dose levels (71). Dosimeter manufacturing procedures are currently under development to minimize this background signal variability.

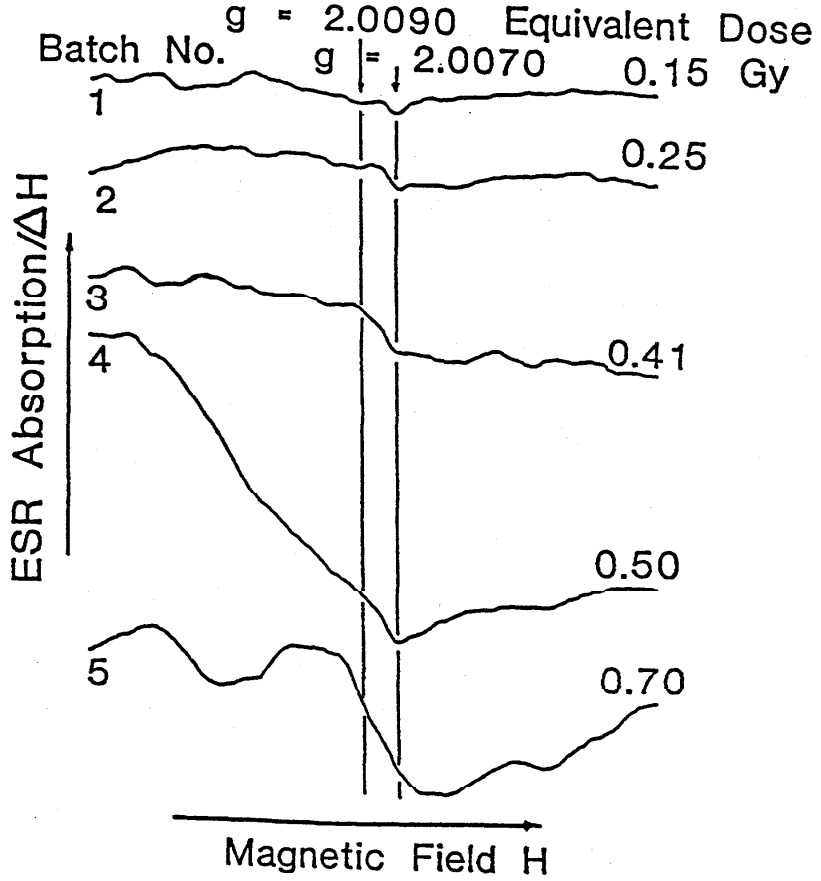

Figure 13. Examples of ESR spectra (total magnetic field scan 20 mT) of unirradiated alanine/paraffin dosimeters from different batches produced in the same laboratory (71). The right-hand numbers indicate the "artefact" equivalent doses represented by the amplitudes of these background spectra.

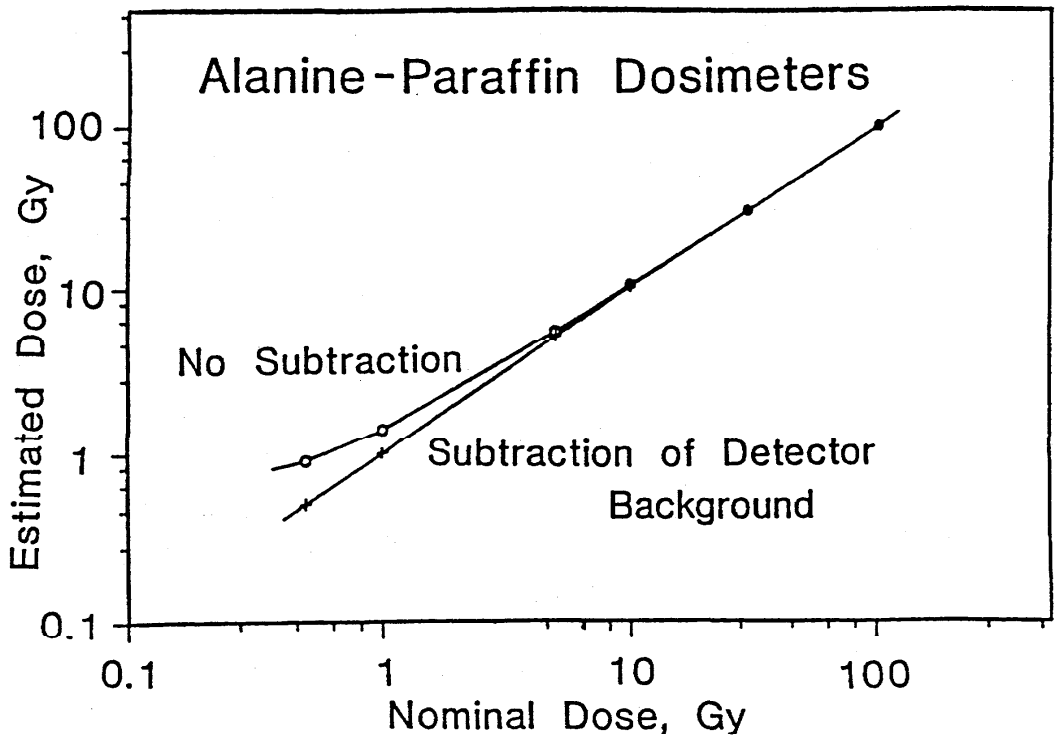

Figure 14. Estimated dose registered by reading irradiated alanine/paraffin dosimeters, as a function of the nominal dose, with and without correction for the kind of background spectral amplitude illustrated in Figure 12 (71). The corrected response (linear log-log function) is normalized according to the calibration at a dose of 1 kGy.

Another concern is the general perception that alanine is "tissue-" or "water-equivalent" in its radiation response characteristics (see Table IV). Figure 15 shows ratios of photon energy absorption coefficients (μ_{en}) and electron collision stopping powers (S_{coll}), alanine-to-water (52). These calculations reveal that absorbed dose in alanine for typical irradiations by ionizing photons and electrons would have values three or four percent lower than the absorbed dose in water. However, when the calibration is made in terms of absorbed dose in water, corrections are required only if the practical irradiations requiring dose measurement (photons or electrons) encounter materials having significantly different absorption properties from those involved in the calibration (41).

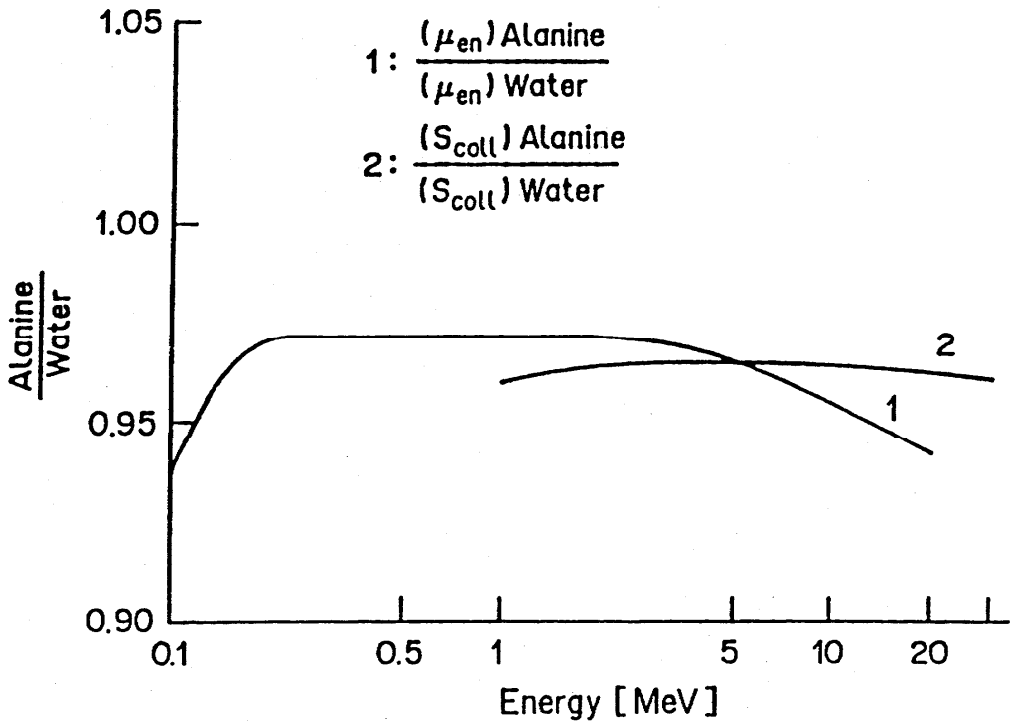

Figure 15. For the spectral regions indicated: Curve 1, ratio of calculated mass energy-absorption coefficients for alanine and water; Curve 2, ratio of calculated mass collision stopping power for alanine and water.

Bone and Tooth Dosimetry

Another broad use of ESR spectrometry for dosimetry involves ESR measurement of irradiated bone or tooth enamel. Applications include the detection and the dose assessment of certain irradiated foods (fish, shell fish, and meats containing bone) (16,17,18,43,55,64), investigations of dose to residents near the Chernobyl reactor (33), measurements of dose to bone in nuclear medicine (19), and the dating of prehistoric human and animal (e.g., mammoth) skulls, their fossils, and of shells from 1000 years to 10 million years old (13,20,26). These specimens have been exposed over millennia to natural background radiation, and, upon further irradiation in the laboratory to a series of known doses, a careful curve fitting allows extrapolation to the time at which exposure to natural radiation began (27). In fact, ESR dating using radiation-induced E′ centers in quartz has been successful with samples that are orders-of-magnitude older than carbonaceous samples that can be dated back to about 60,000 years by radiocarbon dating, namely geological specimens older than one billion years (26,31).

Bone and tooth dosimetry methods are made possible because of the radiation-sensitive and highly stable ESR signal induced in the radical carbonate ion, CO_3^{3-}, present in irradiated hydroxyapatite. Figure 16 shows the radiation-induced ESR spectrum of a beagle bone following radiotherapy treatment by internally administering short-range β radiation from the radionuclide ^{166}Ho (19). A typical ESR spectrum due to the hydroxyapatite center in bone is seen in Figure 17,

for a chicken bone irradiated with ^{60}Co gamma radiation (18). The ESR technique for the detection of irradiated foods is illustrated in Figure 18, and is similar to the use of the standard addition of laboratory doses applied in ESR dating (18). In this example, frog leg bones from two different locations were given the same unknown dose, and after laboratory doses and an exponential least-squares curve fit (17,18) had been applied, the unknown dose of 1 kGy could be identified.

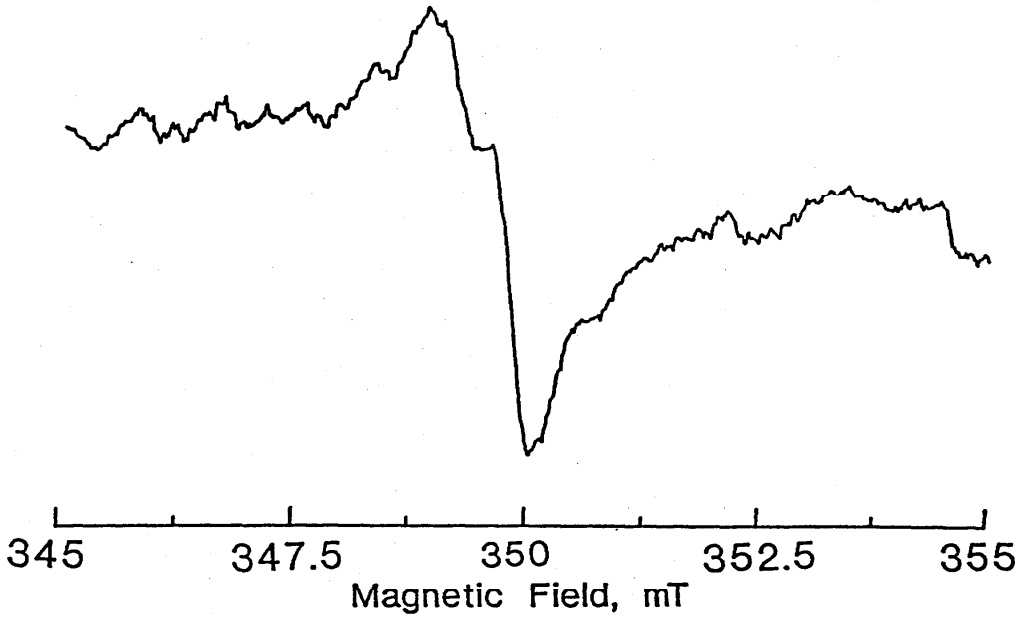

Figure 16. The ESR first-derivative spectrum for a fragment of a humerus cortical bone midshaft from a beagle that had been treated by ^{166}Ho radiotherapy (a low energy β-ray emitter) (19). The estimated dose (measured at 349 mT) is 6 Gy.

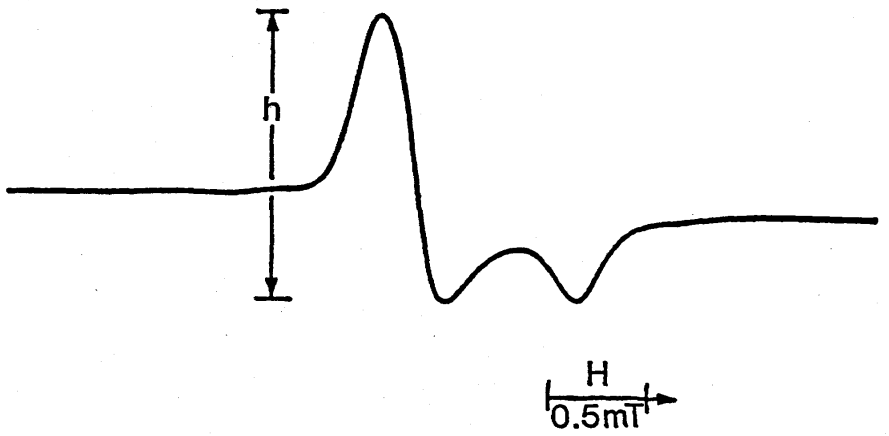

Figure 17. The ESR first-derivative spectrum of a chicken bone irradiated by ^{60}Co gamma radiation (18). Detection of irradiated meat containing bone and evaluation of the dose depend on the functional relationship between the peak-to-peak amplitude, h, and the absorbed dose, established by administering a series of post-irradiation doses.

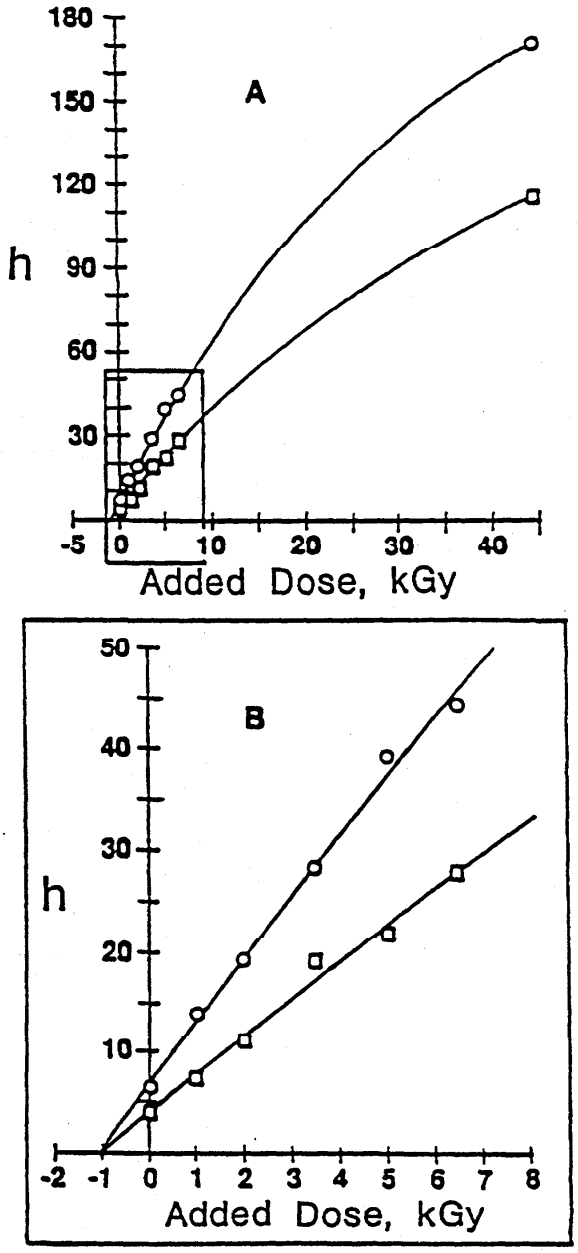

Figure 18. Plots of ESR peak-to-peak amplitude, h, as a function of added dose, for gamma-ray irradiated frog bones (18). The two curves are for two different frog bones given the same initial dose, which is estimated by exponential least-square curve fits to be 1 kGy. The curves in plot B are the enlargements of the boxed area in plot A.

Sugar/ESR Dosimetry

Ordinary granulated sugar (sucrose) has been proposed for use as an emergency dosimeter (67). In fact, post-accident measurements have been made in the dose range of 0.05-40 Gy from household sugar collected from apartments at

different sites near the Chernobyl reactor episode that took place on April 26, 1986 (46,47). This is one of the most sensitive ESR dosimetry systems, and yet one that has a wide dynamic range up to the usual sterilization doses. Figure 19 shows, for a sucrose/paraffin sample, the ESR spectral signal induced by an electron dose of 2.8×10^4 Gy (44). For granulated sugar the response curve shape displays a linear response function between the ESR signal and dose at the lower dose range (see Figure 20). The radiation-induced signal is so stable that the use of sugar pellets may be proposed for broad-range routine dosimetry (66,67). However, some caution should be taken; recent investigations have found that sucrose dosimeter fabrication techniques (e.g., grinding and pressing) may produce free-radical ESR signals identical to the radiation-induced signal (24).

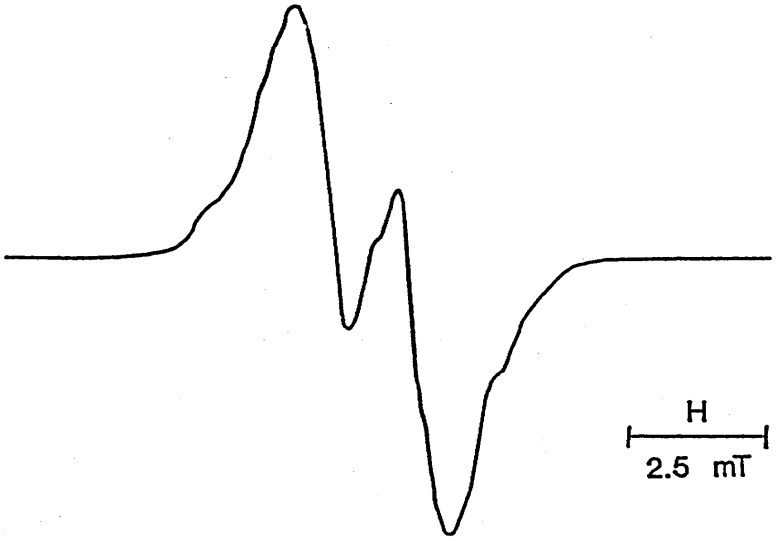

Figure 19. The ESR First-Derivative Spectrum for a Sucrose/Paraffin Sample Irradiated With Electrons From a 4-MeV Accelerator to an Absorbed Dose of 2.8×10^4 Gy (44)

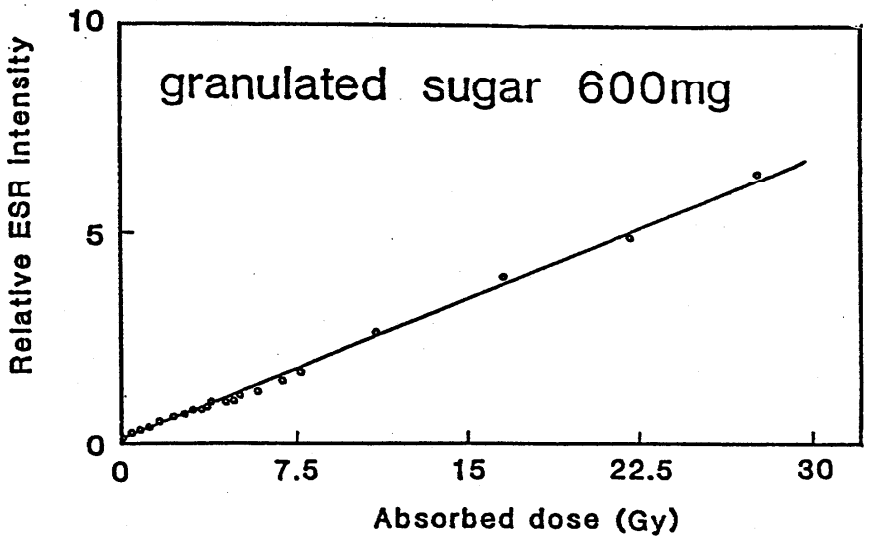

Figure 20. The Response Curve for a 600-mg Sample of Granulated Sugar (Sucrose) Irradiated By ^{60}Co Gamma Radiation (46)

ESR Imaging

The imaging of radiation dose distributions in two and three dimensions by ESR techniques has recently achieved relatively high spatial resolution (22,38,65). The method is similar to nuclear magnetic resonance imaging in that it combines the magnetic field gradients with spectral scanning over spatial ranges along the different spatial axes. The spectral-spatial scanning can be accomplished in either the X- (65) or L-band (38). It generally requires, however, customized controls of magnetic field, frequency, and amplitude modulation, and adaptation of the geometric arrangement in the spectrometer cavity, as well as added sets of gradient coils to generate sustained field gradients in two or three dimensions. This type of imaging also puts extra demands on spectral resolution (line width and its relation to the ESR signal) and the maximizing of field sensitivity for optimizing ESR signal-to-noise through signal averaging.

Profiles of radical concentration with depth due to electron-beam depth-dose penetration have been measured in this way in an alanine-paraffin block or rod dosimeter, and the resulting ESR absorption spectral-spatial images generated (14,44). Figure 21 (top) shows the experimental depth-dose (solid curve) for a degraded spectrum of 4-MeV electrons incident on the end of a 10-mm long dosimeter block along with the calculated depth-dose (dashed curve) for monoenergetic 4-MeV electrons incident on a semi-infinite material (44). At the bottom of the figure is a spectral-spatial 2-D image, where the ESR signal intensity is vertical (z axis), the depth-dose profile goes from back-to-front (y axis), and the magnetic sweep from left-to-right (x axis). For 2-D spatial imaging, another method is to use multiple sweeps and, by changing slightly the field direction for each sweep in the x-y dimensional plane of the test object, signal deconvolution can be made for all projections (29,30). This computerized tomographic method using multiple projections gives 2-D ESR images such as that shown in Figure 22 for a quartz glass tube irradiated by an isotropic field of ^{60}Co gamma radiation (73). Relatively high spatial resolution in two and three dimensions can now be generated in a number of irradiated substances, such as alanine dosimeters or bone samples (29,30,38,44).

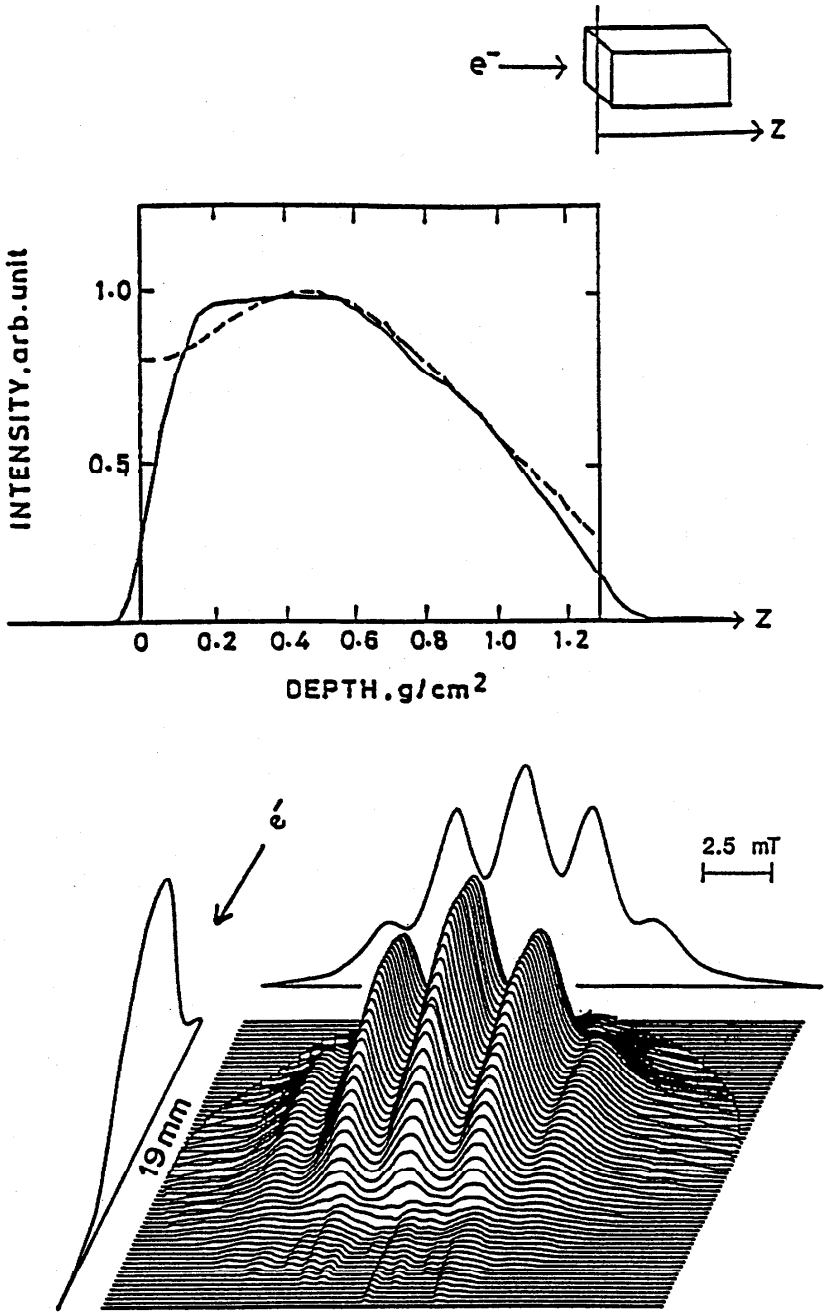

Figure 21. (Top) Calculated (dashed curve) and ESR-measured (solid curve) depth-dose profile for a 4-MeV electron beam incident from the left on a dosimeter block of alanine/paraffin (upper right inset) (44); (Bottom) the spectral-spatial image of the ESR absorption spectrum relative amplitude (vertical scale) as a function of penetration depth in the block (back-to-front). The absorbed dose at the maximum of the depth-dose curve was 2.8×10^4 Gy.

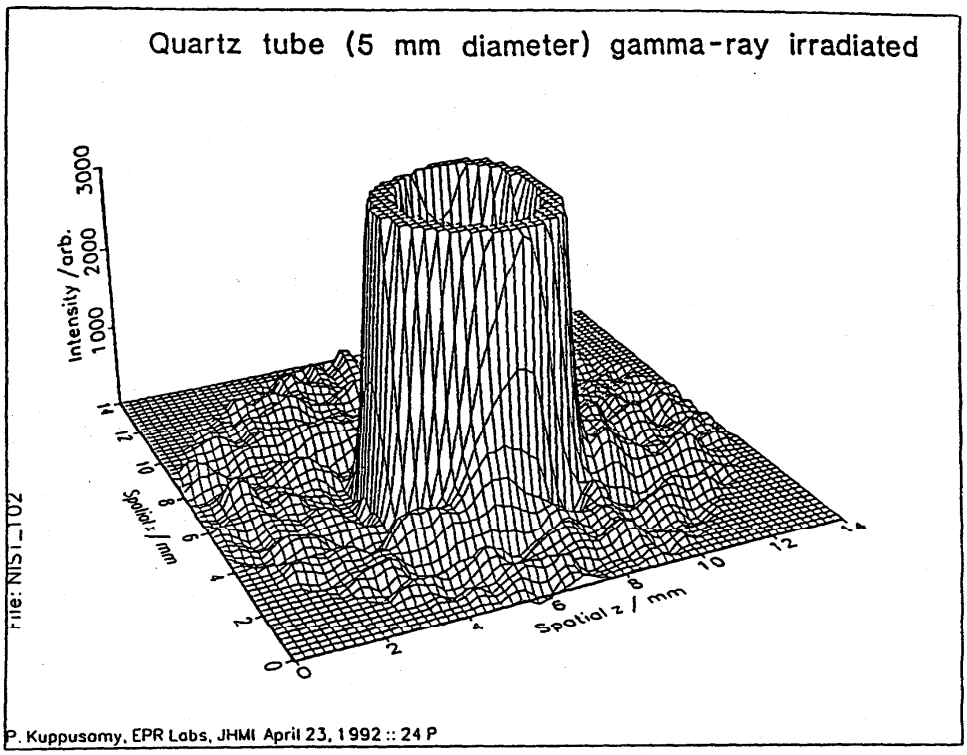

Figure 22. A two-dimensional (2-D; x-z coordinates) image of a quartz tube irradiated uniformly by an annular ^{60}Co gamma-ray source arrangement around the axis of the tube (73). The vertical scale shows the relatively uniform distribution of the ESR intensity registered with a spatial resolution of 0.222 mm per division.

Summary

Electron spin resonance (ESR) spectrometry has attracted attention in radiation processing. Not only is ESR analysis of alanine achieving success as a reference dosimetric system, but ESR also provides a means of evaluating short- and long-term effects of radiation on polymers, composites and ceramics, and in the post-irradiation analysis and imaging of absorbed dose in teeth and bone. The broad range of doses ($10^{-1}-10^{8}$ Gy) and dose rates (up to 10^{8} Gy s^{-1}) measurable with relatively high precision and accuracy, and the small size, ruggedness, and the expected inexpensiveness of new sensor materials, such as L-α-alanine pellets and films and other sensor materials (e.g., hydroxyapatite, sugar, quartz, cellulose, etc.), make ESR dosimetry attractive for radiation sterilization dosimetry, radiation treatment planning, nuclear medicine dosimetry, food irradiation, and the study of radiation effects on materials. Within the next few years, there may be a significant impact of this ESR-based analysis on international radiation standards practices and 2-D and 3-D imaging of radiation dose distributions, especially as the trend toward lowering the cost of the analytical equipment and simplifying its operation continues (20). ESR dosimetry may, in fact, be the future method of choice for inter-laboratory transfer metrology, process validation, and measurement quality assurance.

Profound improvements in the practice of alanine/ESR dosimetry are currently being made. Mass-produced batches of rugged, low-cost alanine dosimeters are now on the threshold of becoming commercially available. There are also advanced, easy-to-use ESR spectrometers designed especially for dosimetry and requiring no manual instrumental adjustments or tedious dosimeter manipulations. New spectrometer capabilities may be summarized as follows: automated dosimeter transport, positioning, and changing; microprocessor-controlled reproducible instrument settings to minimize instrumental drifts (e.g., RF frequency control, microwave bridge tuning, detector bias current setting); continuous measurement and high sample throughput (as high as 400 dosimeter readings per hour); and automated data logging, evaluation of dosimeter results, and calibration history recall. These developments should result in greater dosimetric precision, ease of use, and cost effectiveness for large-scale dosimetry applied to radiation processing.

References

1. Aldrich JE, Pass B. Determining radiation exposure from nuclear accidents and atomic tests using dental enamel. Health Phys 1988;54:469-471.
2. Alger RS. *Paramagnetic Resonance Techniques and Application.* New York: Interscience; 1968; 13-15.
3. Arnow CL. Benchtop ESR spectrometer 8200 utilizes permanent magnet. Skokie, IL: Micronow Instruments Report; Nov. 1991.
4. Azorin J, Gutiérrez A, Muñoz E, Gleason R. Correlation of ESR with lyoluminescence dosimetry using some sugars. Appl Radiat Isotopes 1989;40:871-873.
5. Baccarlo S, Buontempo U, Caccia B, Onori S, Puntaloni M. ESR study of irradiated ethylene-propylene rubber. Appl Radiat Isotopes 1993;44:331-335.
6. Bermann F, DeChoudens H, Descours S. Application à la dosimetrie de la mesure par resonance paramagnétique électronique des radicaus libre créés dans les acides amines. *Advances in Physical and Biological Radiation Detectors*, STI/PUB/269. Proceedings of Symposium, Vienna 1970, Vienna: IAEA; 1971; 311-325.
7. Bradshaw WW, Cadena CG, Crawford EW, Spetzler HAW. The use of alanine as a solid dosimeter. Radiat Res 1962;17:11-21.
8. Bortolin E, Fattibene P, Furetta C, Onori S. ESR of Mg_2SiO_4:Tb TL phosphor. Appl Radiat Isotopes 1993;44:327-330.
9. Box HC, Freund HG. Paramagnetic resonance shows radiation effects. Nucleonics 1959;17(1):66-76.
10. Bushfield KW, Garrett RW, Hill DJT, O'Donnell JH, Pommery PJ. Detection of intermediates in irradiated polymers by electron spin resonance spectroscopy. Polymer Preprints 1988;29:126-127.
11. Chien JCW, Boss CR. Electron spin resonance spectra of low molecular weight and high molecular weight peroxy radicals. J Am Chem Soc 1967;89:571-575.
12. Chien JCW, Boss CR. Polymer reactions. V. Kinetics of auto-oxidation of polypropylene. J Polymer Sci Past A1 1967;5:3091-3101.
13. Chong TS, Ohta H, Nakashima Y, Iida T, Ieda K, Saisho H. ESR dating of elephant teeth and radiation dose rate estimation in soil. Appl Radiat Isotopes 1989;40:1199-1202.
14. Colacicchi S, Onori S, Petetti E, Sotgiu A. Application of low frequency EPR imaging to alanine dosimetry. Appl Radiat Isotopes 1993;44:391-395.

15. Coninckx F, Schönbacher H. Experience with a new polymer-alanine dosimeter in high energy particle accelerator environment. Appl Radiat Isotopes 1993;44:67-71.
16. Desrosiers MF. Gamma-irradiated seafoods: Identification and dosimetry by electron paramagnetic resonance spectroscopy. J Agric Food Chem 1989;37:96-100.
17. Desrosiers MF. Estimation of the absorbed dose in radiation processed food — 2. Test of the EPR response function by an exponential fitting analysis. Appl Radiat Isotopes 1991;42:617-619.
18. Desrosiers MF, McLaughlin WL, Sheahan LA, et al. Co-trial on ESR identification and estimates of γ-ray and electron absorbed dose given to meat and bones. Int J Food Sci Technol 1990;25:682-691.
19. Desrosiers MF, Avila MJ, Schauer DA, Coursey BM, Parks NJ. Experimental validation of radiopharmaceutical absorbed dose to mineralized bone tissue. Appl Radiat Isotopes 1993;44:459-463.
20. Desrosiers MF, Skinner AF (Eds.) *ESR Dosimetry and Applications*. Proceedings of 3rd International Symposium, Gaithersburg, MD. 1991; Appl Radiat Isotopes 1993;44:1-468.
21. Desrosiers MF, Puhl JM, McLaughlin WL. A new EPR dosimeter based on polyvinylalcohol. Appl Radiat Isotopes 1993;44:325-326.
22. Eaton GR, Eaton SS, Ohno K (eds.) *EPR Imaging and* in vivo *EPR*. Boca Raton, FL: CRC Press; 1991.
23. Ettinger KV, Eid AM, Forrester AR. Electron spin resonance readout for LiF dosemeters. Radiat Prot Dosimetry 1983;6:166-168.
24. Fattibene P, Desrosiers MF. NIST Gaithersburg 1993; Private communication.
25. Feist H, Regulla D, Wieser A. Is alanine/ESR dosimetry now an alternative to ferrous sulfate dosimetry? Appl Radiat Isotopes 1993;44:47-51.
26. Grün R. Present status of ESR dating. Appl Radiat Isotopes 1989;40:1045-1055.
27. Grün R, MacDonald PDM. Non-linear fitting of TL/ESR dose-response curves. Appl Radiat Isotopes 1989;40:1077-1080.
28. Harrah, LA. ESR of radicals produced in Co-60 gamma-irradiated polystyrene. In: Adler G, ed. *Organic Solid State Chemistry*. New York: Gordon and Breach; 1969; 197-210.
29. Hochi A, Furusawa M, Ikeya M. Applications of microwave scanning ESR microscope: Human tooth with metal. Appl Radiat Isotopes 1993;44:401-405.
30. Ikeya M. Scanning and computer tomography — ESR microscopy. In: Blümich B, Kuhn W, eds. *Magnetic Resonance Microscopy*. Weinheim: VCH Verlagsgesellschaft; 1992; 133-149.
31. Ikeya M. From earth to space: ESR dosimetry moves toward the 21st century. Appl Radiat Isotopes 1993;43:1-5.
32. Ikeya M, Miki T, eds. *ESR Dating and Dosimetry*, Proceedings of 1st International Symposium, Yamaguchi; Tokyo: Ionics; 1985.
33. Ishii H, Ikeya M, Okano M. ESR dosimetry of teeth of residents close to Chernobyl reactor accident. J Nucl Sci Technol 1990;27:1153-1155.
34. Janovsk L. Progress in alanine film/ESR dosimetry. *High Dose Dosimetry for Radiation Processing*, STI/PUB/846. Proceedings of Symposium, Vienna 1990. Vienna: IAEA; 1991;173-187.
35. Judeikis HS, Hedgpeth H, Siegal S. Free radical yields in polytetrafluoroethylene as the basis for a radiation dosimeter. Radiat Res 1968;35:247-260.
36. Kojima T, Tanaka R. Polymer-alanine dosimeter and compact reader. Appl Radiat Isotopes 1989;40:851-857.
37. Kojima T, Haruyama Y, Tachibana H, et al. Development of portable ESR spectrometer as a reader for alanine dosimeters. Appl Radiat Isotopes 1993;44:361-365.

38. Kuppusamy P, Chzhan M, Vij K, et al. 3-D spectral-spatial EPR imaging of free radicals in the heart: A technique for *in vivo* imaging of tissue metabolism and oxygenation. Proceedings of National Academy of Sciences. Washington: NAS; 1993;90-111.
39. Kuroda S, Miyagawa I. ENDOR study of an irradiated crystal of L-alanine: Environment of the stable $CH_3\dot{C}HCO_2^-$ radical. J Chem Phys 1982;76:3933-3944.
40. Maier D, Schmalbein D. A dedicated EPR analyzer for dosimetry. Appl Radiat Isotopes 1993;44:345-355.
41. McLaughlin WL. ESR dosimetry. Radiat Prot Dosimetry 1993; 46 (in press).
42. McLaughlin WL, Boyd AW, Chadwick KH, McDonald JC, Miller A. *Dosimetry for Radiation Processing*. London: Taylor and Francis; 1989; 173-176, 190, 200.
43. Morehouse K, Desrosiers MF. Electron spin resonance investigations of gamma-irradiated shrimp shell. Appl Radiat Isotopes 1993;44:429-437.
44. Morita Y, Ohno K, Ohashi K, Sohma J. ESR imaging investigation on depth profiles of radicals in organic solid dosimetry. Appl Radiat Isotopes 1989;40:1237-1232.
45. Morton JR, Schneider CCJ. ESR dosimetry with magnesium sulfate. Radiat Prot Dosimetry 1993; 46 (in press).
46. Nakajima T. Sugar as an emergency populace dosimeter for radiation accidents. Health Phys 1988;55:951-955.
47. Nakajima T. Estimation of absorbed dose to evacuees at Pripyat-City using ESR measurements of sugar and exposure rate calculations. Appl Radiat Isotopes 1993;44 (in press).
48. Nam JW, Regulla DF. The significance of the International Dose Assurance Service for radiation processing. Appl Radiat Isotopes 1989;40:953-955.
49. Nette HP, Onori S, Fattibene P, Regulla DF, Wieser A. Coordinated research efforts for establishing an International Radiotherapy Dose Intercomparison Service based on the alanine/ESR system. Appl Radiat Isotopes 1993;44:7-11.
50. Nishimoto S-I, Mu Ye, Yiqun Lu, Kawamura T, Kagiya T. ESR spectroscopic characterization of the methyl viologen dosimeter in poly (vinyl alcohol) film. Radiat Phys Chem 1988;322:727-730.
51. O'Donnell JH, Pommery PJ. ESR studies of degradation in polymers. I. γ-irradiation of poly (styrene-co-methyl methacrylate) at 77° K. J Polym Sci, Symposium No. 55 1976: 269-278.
52. Olsen KJ, Hansen JW, Waligorski MPR. ESR dosimetry in calibration intercomparisons with high energy photons and electrons. Appl Radiat Isotopes 1989;40:985-988.
53. Oommen IK, Nambi KSV, Sengupta S, Gundu Rao TK, Ravikumar M. Lactose and "Tris" lyoluminescence dosimetry systems and ESR correlation studies. Appl Radiat Isotopes 1989;40:879-883.
54. Pass B, Aldrich JE. Dental enamel as an *in vivo* radiation dosimeter. Med Phys 1985;12:305-307.
55. Raffi J, Evans JC, Agnel J-OL, Rowlands CC, Lesgards G. ESR analysis of irradiated frogs legs and fishes. Appl Radiat Isotopes 1989;40:1215-1218.
56. Regulla DF, Deffner U. Dosimetry by ESR spectroscopy of alanine. In: McLaughlin WL, ed. *Trends in Radiation Dosimetry*. Oxford: Pergamon Press; Int J Appl Radiat Isotopes 1982;33:1101-1114.
57. Regulla DF, Deffner U. A system of transfer dosimetry in radiation processing. Radiat Phys Chem 1983;22:305-309.
58. Regulla DF, Scharmann A, McLaughlin WL, eds. *ESR Dosimetry and Applications*, Proceedings of 2nd International Symposium, Munich, 1988; Appl Radiat Isotopes 1989;40:829-1246.
59. Regulla D, Bartalotta A, Deffner U, Onori S, Pantaloni M, Wieser A. Calibration network based on alanine/ESR dosimetry. Appl Radiat Isotopes 1993;44:23-31.

60. Rotblat J, Simmons JA. Dose-response relationship in the yield of radiation-induced free radicals in amino acids. Phys Med Biol 1963;7:489-497.
61. Sharpe PHG, Arber JM. Fading characteristics of irradiated alanine pellets: The importance of pre-irradiation conditioning. Appl Radiat Isotopes 1993;44:19-22.
62. Sollier TJL, Mosse DC, Chartier MMT, Joli JE. The LMRI ESR/alanine dosimetry system: description and performance. Appl Radiat Isotopes 1989;40:961-965.
63. Stachowicz W, Burlińska G, Michalik J, Dziedzic-Goclawska A, Ostrowski K. Applications of the EPR spectroscopy to radiation-treated materials in medicine, dosimetry, and agriculture. Appl Radiat Isotopes 1993;44:423-427.
64. Stewart EM, Stevenson NH, Gray R. Detection of irradiation in scampi tails — Effects of sample preparation, irradiation dose and storage on ESR response of the cuticle. Int J Food Sci Technol 1992;27:125-132.
65. Sueki M, Eaton SS, Eaton GR. Spectral-spatial EPR imaging of irradiated silicon dioxide. Appl Radiat Isotopes 1993;44:377-380.
66. Tchien A, Greenstock CL, Trivedi A. The use of sugar pellets in ESR dosimetry. Radiat Prot Dosimetry 1993;46:191-201.
67. Trivedi A, Greenstock CL. Use of sugars and hair for ESR emergency dosimetry. Appl Radiat Isotopes 1993;44:85-90.
68. Uribe RM, McLaughlin WL, Miller A, Dunn TS, Williams EE. Possible use of electron spin resonance of polymer films containing leucodyes for dosimetry. Radiat Phys Chem 1981;18:1011-1016.
69. Wieser A, Regulla, DF. ESR Dosimetry in the "gigarad" range. Appl Radiat Isotopes 1989;40:911-913.
70. Wieser A, Regulla, DF. Cellulose for high-level dosimetry. *High-Dose Dosimetry for Radiation Processing*, STI/PUB/846. Proceedings of International Symposium, Vienna 1990. Vienna: IAEA; 1991; 203-212.
71. Wieser A, Lettan C, Fill U, Regulla DF. The influence of non-radiation induced ESR background signal from paraffin-alanine probes for dosimetry in the radiotherapy range. Appl Radiat Isotopes 1993;44:59-65.
72. Williams JL, Dunn TS, Sugg H, Stannett V. Radiation stability of polypropylene. Radiat Phys Chem 1977;9:445-554.
73. Figure courtesy of Zweier JL, Kuppusamy P, Schauer DA. EPR Laboratories and Department of Medicine. The Johns Hopkins University School of Medicine, Francis Scott Key Medical Center, Baltimore, Maryland.